

# Training behavior of deep neural network in frequency domain<sup>\*</sup>

Zhi-Qin John Xu<sup>\*\*1</sup>, Yaoyu Zhang<sup>2</sup>, and Yanyang Xiao<sup>2</sup>

<sup>1</sup> School of Mathematical Sciences and Institute of Natural Sciences, Shanghai Jiao Tong University, Shanghai, China,

[xuzhiqin@sjtu.edu.cn](mailto:xuzhiqin@sjtu.edu.cn),

<sup>2</sup> School of Mathematics, Institute for Advanced Study, Princeton, NJ 08540, USA, [yaoyu@ias.edu](mailto:yaoyu@ias.edu),

<sup>3</sup> The Brain Cognition and Brain Disease Institute, Shenzhen Institutes of Advanced Technology, Chinese Academy of Sciences, China, [xyy82148@gmail.com](mailto:xyy82148@gmail.com)

**Abstract.** Why deep neural networks (DNNs) capable of overfitting often generalize well in practice is a mystery [24]. To find a potential mechanism, we focus on the study of implicit biases underlying the training process of DNNs. In this work, for both real and synthetic datasets, we empirically find that a DNN with common settings first quickly captures the dominant low-frequency components, and then relatively slowly captures the high-frequency ones. We call this phenomenon Frequency Principle (F-Principle). The F-Principle can be observed over DNNs of various structures, activation functions, and training algorithms in our experiments. We also illustrate how the F-Principle helps understand the effect of early-stopping as well as the generalization of DNNs. This F-Principle potentially provides insight into a general principle underlying DNN optimization and generalization.

**Keywords:** Deep Neural Network · Deep Learning · Fourier analysis · Generalization.

## 1 Introduction

Although Deep Neural Networks (DNNs) are totally transparent, i.e., the value of each node and each parameter can be easily obtained, it is difficult to interpret how information is processed through DNNs. We can easily record the trajectories of the parameters of DNNs during the training. However, it remains unclear what is the general principle underlying the highly non-convex problem of DNN optimization [9]. Therefore, DNN is often criticized for being a “black box” [1,18]. Even for the simple problem of fitting one-dimensional (1-d) functions, the training process of DNN is still not well understood [16,19]. For example, Wu et al.

---

<sup>\*</sup> Originally submitted to arxiv.org on 3 Jul 2018. To appear in 2019 26th-International conference of neural information processing (ICONIP).

<sup>\*\*</sup> Corresponding author

(2017) [19] use DNNs of different depth to fit a few data points sampled from a 1-d target function of third-order polynomial. They find that, even when a DNN is capable of over-fitting, i.e., the number of its parameters is much larger than the size of the training dataset, it often generalizes well (i.e., no overfitting) after training. In practice, the same phenomenon is also observed for much more complicated datasets [7,11,28,24,10,19]. Intuitively, for a wide DNN, its solutions of zero training error lies in a huge space where well-generalized ones only occupy a small subset. Therefore, it is mysterious that DNN optimization often ignores a huge set of over-fitting solutions. To find an underlying mechanism, in this work, we characterize the behavior of the DNN optimization process in the frequency domain using 1-d functions as well as real datasets of image classification problems (MNIST and CIFAR10). Our work provides insight into an implicitly bias underlying the training process of DNNs.

We empirically find that, for real datasets or synthetic functions, a DNN with common settings first quickly captures their dominant low-frequency components while keeping its own high-frequency ones small, and then relatively slowly capture their high-frequency components. We call this phenomenon *Frequency Principle* (F-Principle). From our numerical experiments, this F-Principle can be widely observed for DNNs of different width (tens to thousands of neurons in each layer), depth (one to tens of hidden layers), training algorithms (gradient descent, stochastic gradient descent, Adam) and activation functions (tanh and ReLU). Remark that this strategy of the F-Principle, i.e., fitting the target function progressively in ascending frequency order, is also adopted explicitly in some numerical algorithms to achieve remarkable efficiency. These numerical algorithms include, for example, the Multigrid method for solving large-scale partial differential equations [5] and a recent numerical scheme that efficiently fits the three-dimensional structure of proteins and protein complexes from noisy two-dimensional images [3].

The F-Principle provides a potential mechanism of why DNNs often generalize well empirically albeit its ability of over-fitting [24]. For a finite training set, there exists an effective frequency range [17,23,12] beyond which the information of the signal is lost. By the F-Principle, with no constraint on the high-frequency components beyond the effective frequency range, DNNs tend to keep them small. For a wide class of low-frequency dominant natural signals (e.g., image and sound), this tendency coincides with their behavior of decaying power at high frequencies. Thus, DNNs often generalize well in practice. When the training data is noisy, the small-amplitude high-frequency components are easier to be contaminated. By the F-Principle, DNNs first capture the less noisy low-frequency components of the training data and keep higher-frequency components small. At this stage, although the loss function is not best optimized for the training data, DNNs could generalize better for not fitting the noise dominating the higher-frequencies. Therefore, as widely observed, early-stopping often helps generalization.

Our key contribution in this work is the discovery of an F-Principle underlying the training of DNNs for both synthetic and real datasets. In addition, we

demonstrate how the F-Principle provides insight into the effectiveness of early stopping and the good generalization of DNNs in general.

## 2 Related works

Consistent with other studies [19,2], our analysis shows that over-parameterized DNNs tend to fit training data with low-frequency functions, which are naturally of lower complexity. Intuitively, lower-frequency functions also possess smaller Lipschitz constants. According to the study in Hardt et al. (2015) [6], which focuses on the relation between stability and generalization, smaller Lipschitz constants can lead to smaller generalization error.

The F-Principle proposed in this work initiates a series of works [22,20,21,14,27,25,4]. A stronger verification of the F-Principle for the high dimensional datasets can be found in Xu et al., (2019) [21]. Theoretical studies on the F-Principle can be found in Xu et al., (2019), Xu et al., (2019) and Zhang et al., (2019) [22,21,25]. The F-Principle is also used as an important phenomenon to pursue fundamentally different learning trajectories of meta-learning [14]. The theoretical framework [22,21] of analyzing the F-Principle is used to analyze a nonlinear collaborative scheme for deep network training [27]. Based on the F-Principle, a fast algorithm by shifting high frequencies to lower ones is developed for fitting high frequency functions [4]. These subsequent works show the importance of the F-Principle.

## 3 Experimental setup

We summarize the setups for each figure as follows. All DNNs are trained by the Adam optimizer, whose parameters are set to their default values [8]. The loss function is the mean-squared error. The parameters of DNNs are initialized by a Gaussian distribution with mean 0.

In Fig. 1, the setting of the fully-connected tanh-DNN is as follows. Width of hidden layers: 200-100-100; Batch size: 100; Learning rate:  $10^{-5}$  for CIFAR10 and  $10^{-6}$  for MNIST; Standard deviation of Gaussian initialization:  $10^{-4}$ . The setting of the ReLU-CNN is as follows: two layers of 32 features with  $3 \times 3$  convolutional kernel and  $2 \times 2$  max-pooling, followed by 128-64 densely connected layers; Batch size: 128; Standard deviation of Gaussian initialization: 0.05. We select 10000 samples from each dataset for the training.

In Figs. (2, 3, 4, 5), we use a fully-connected tanh-DNN of 4 hidden layers of width 200-200-200-100, standard deviation of Gaussian initialization 0.1, learning rate  $2 \times 10^{-5}$  and full-batch size training.

In addition,  $\mathcal{F}[\cdot]$  indicates the Fourier transform, which is experimentally estimated on discrete training or test data points.

## 4 F-Principle

In this section, we study the training process of DNNs in the frequency domain. We empirically find that, for a general class of functions dominated by low-frequencies, the training process of DNNs follows the F-Principle by which low-frequency components are first captured, followed by high-frequency ones.

### 4.1 MNIST/CIFAR10

Since the computation of high-dimensional Fourier transform suffers from the curse of dimensionality, to verify the F-Principle in the image classification problems (MNIST and CIFAR10), we perform the Fourier analysis along the first principle component of the training inputs.

The training set is a list of labeled images denoted by  $\{\mathbf{x}_k; y_k\}_{k=0}^{n-1}$ , where each image  $\mathbf{x}_k \in [0, 1]^{N_{in}}$ ,  $N_{in}$  is the number of pixels of an image, each label  $y_k \in \{0, 1, 2, \dots, 9\}$ . We use DNNs of two structures to learn this training set, that is, a fully-connected DNN and a CNN. Denote  $x_k = \mathbf{x}_k \cdot \mathbf{v}_{PC}$ , which is the projection of image  $\mathbf{x}_k$  along the direction of the first principle component of  $\{\mathbf{x}_k\}_{k=0}^{n-1}$  denoted by a unit vector  $\mathbf{v}_{PC}$ . Using non-uniform Fourier transform, we obtain

$$\mathcal{F}_{PC}^n[y](\gamma) = \frac{1}{n} \sum_{j=0}^{n-1} y_j \exp(-2\pi i x_j \gamma),$$

where  $\gamma \in \mathbb{Z}$  is the *frequency index*. For the DNN output  $T(\mathbf{x}_k)$ , similarly,  $\mathcal{F}_{PC}^n[T](\gamma) = \frac{1}{n} \sum_{j=0}^{n-1} T(\mathbf{x}_j) \exp(-2\pi i x_j \gamma)$ . To examine the convergence behavior of different frequency components during the training of a DNN, we compute the relative difference of  $\mathcal{F}_{PC}^n[T][\gamma]$  and  $\mathcal{F}_{PC}^n[y][\gamma]$  at each recording step, i.e.,

$$\Delta_F(\gamma) = \frac{|\mathcal{F}_{PC}^n[y](\gamma) - \mathcal{F}_{PC}^n[T](\gamma)|}{|\mathcal{F}_{PC}^n[y](\gamma)|}, \quad (1)$$

where  $|\cdot|$  denotes the absolute value. As shown in the first column in Fig. 1, both datasets are dominated by low-frequency components along the first principle direction. Theoretically, frequency components other than the peaks are susceptible to the artificial periodic boundary condition implicitly applied in the Fourier transform, thereby are not essential to our frequency domain analysis [13]. In the following, we only focus on the convergence behavior of the frequency peaks during the training. By examining the relative error of certain selected key frequency components (marked by black squares), one can clearly observe that DNNs of both structures for both datasets tend to capture the training data in an order from low to high frequencies as stated by the F-Principle<sup>4</sup> (second and third column in Fig. 1).

<sup>4</sup> Almost at the same time, another research [15] finds a similar result. However, they add noise to MNIST, which contaminates the labels.

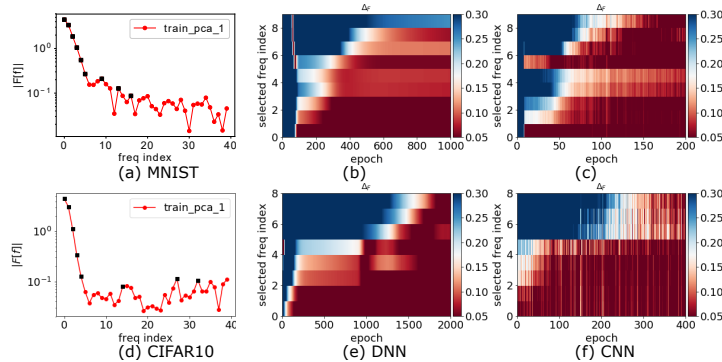


**Fig. 1.** Frequency analysis of DNN output function along the first principle component during the training. The training datasets for the first and the second row are from MNIST and CIFAR10, respectively. The neural networks for the second column and the third column are fully-connected DNN and CNN, respectively. (a,d)  $|\mathcal{F}_{PC}^1[y](\gamma)|$ . The selected frequencies are marked by black dots. (b, c, e, f)  $\Delta_F$  at different recording epochs for different selected frequencies.  $\Delta_F$  larger than 0.3 (or smaller than 0.05) is represented by blue (or red).

## 4.2 Synthetic data

In this section, we demonstrate the F-Principle by using synthetic data sampled from a target function of known intrinsic frequencies. We design a target function by discretizing a smooth function  $f_0(x)$  as follows,

$$y = f(x) = \alpha \times \text{Round}(f_0(x)/\alpha), \quad \alpha \in (0, \infty), \quad (2)$$

where  $\text{Round}(\cdot)$  takes the nearest integer value. We define  $y = f_0(x)$  for  $\alpha = 0$ . We consider  $f_0(x) = \sin(x) + 2 \sin(3x) + 3 \sin(5x)$  with  $\alpha = 2$  as shown in Fig. 2a. As shown in Fig. 2b, for the discrete Fourier transform (DFT) of  $f(x)$ , i.e.,  $\mathcal{F}[f]$ , there are three most important frequency components and some small peaks due to the discretization. In this case, we can observe a precise convergence order from low- to high-frequency for frequency peaks as shown in Fig. 2c.

We have performed the same frequency domain analysis for various low-frequency dominant functions, such as  $f_0(x) = |x|$ ,  $f_0(x) = x^2$  and  $f_0(x) = \sin(x)$  with different  $\alpha$ 's (results are not shown), for both ReLU and tanh activation functions, and both gradient descent and Adam [8] optimizers. We find that F-Principle always holds during the training of DNNs. Therefore, the F-Principle seems to be an intrinsic character of DNN optimization.

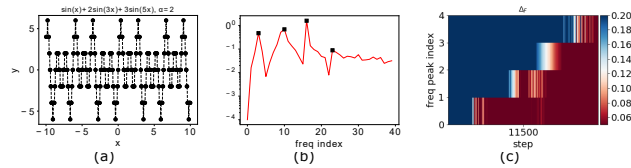


**Fig. 2.** Frequency domain analysis of the training process of a DNN for  $f_0(x) = \sin(x) + 2\sin(3x) + 3\sin(5x)$  with  $\alpha = 2$  in Eq. (2). (a) The target function. (b)  $|\mathcal{F}[f]|$  at different frequency indexes. First four frequency peaks are marked by black dots. (c)  $\Delta_F$  at different recording steps for different frequency peaks. The training data is evenly sampled in  $[-10, 10]$  with sample size 600.

## 5 Understanding the training behavior of DNNs by the F-Principle

In this section, we provide an explanation based on the F-Principle of why DNNs capable of over-fitting often generalize well in practice [7,11,28,24,10,19]. For a class of functions dominated by low frequencies, with finite training data points, there is an *effective frequency range* for this training set, which is defined as the range in frequency domain bounded by Nyquist-Shannon sampling theorem [17] when the sampling is evenly spaced, or its extensions [23,12] otherwise. When the number of parameters of a DNN is greater than the size of the training set, the DNN can overfit these sampling data points (i.e., training set) with different amount of powers outside the effective frequency range. However, by the F-Principle, the training process will implicitly bias the DNN towards a solution with a low power at the high-frequencies outside the effective frequency range. For functions dominated by low frequencies, this bias coincides with their intrinsic feature of low power at high frequencies, thus naturally leading to a well-generalized solution after training. By the above analysis, we can predict that, in the case of insufficient training data, when the higher-frequency components are not negligible, e.g., there exists a significant frequency peak above the effective frequency range, the DNN cannot generalize well after training.

In another case where the training data is contaminated by noise, early-stopping method is usually applied to avoid overfitting in practice [10]. By the F-Principle, early-stopping can help avoid fitting the noisy high-frequency components. Thus, it naturally leads to a well-generalized solution. We use the following example for illustration.

As shown in Fig. 3a, we consider  $f_0(x) = \sin(x)$  with  $\alpha = 0.5$  in Eq. (2). For each sample  $x$ , we add a noise  $\epsilon$  on  $f_0(x)$ , where  $\epsilon$  follows a Gaussian distribution with mean 0 and standard deviation 0.1. The DNN can well fit the sampled training set as the loss function of the training set decreases to a very small value (green stars in Fig. 3b). However, the loss function of the test set first decreases and then increases (red dots in Fig. 3b). That is, the generalization performance of the DNN gets worse during the training after a certain step. In Fig. 3c,  $|\mathcal{F}[f]|$  for the training data (red) and the test data (black) only over-

lap around the dominant low-frequency components. Clearly, the high-frequency components of the training set are severely contaminated by noise. Around the turning step — where the best generalization performance is achieved, indicated by the green dashed line in Fig. 3b — the DNN well captures the dominant peak as shown in Fig. 3c. After that, clearly, the loss function of the test set increases as DNN start to capture the higher-frequency noise (red dots in Fig. 3b). These phenomena conform with our analysis that early-stopping can lead to a better generalization performance of DNNs as it helps prevent fitting the noisy high-frequency components of the training set.

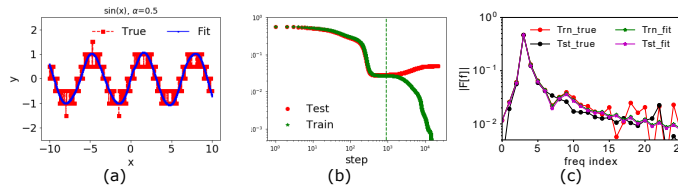


**Fig. 3.** Effect of Early-stopping on contaminated data. The training set and the test set consist of 300 and 6000 data points evenly sampled in  $[-10, 10]$ , respectively. (a) The sampled values of the test set (red square dashed line) and DNN outputs (blue solid line) at the turning step. (b) Loss functions for training set (green stars) and test set (red dots) at different recording steps. The green dashed line is drawn at the turning step, where the best generalization performance is achieved. (c)  $|\mathcal{F}[f]|$  for the training set (red) and test set (black), and  $|\mathcal{F}[T]|$  for the training set (green), and test set (magenta) at the turning step.

## 6 Conclusions and discussion

In this work, we empirically discover an F-Principle underlying the optimization process of DNNs. Specifically, for functions with dominant low-frequency components, a DNN with common settings first capture their low-frequency components while keeping its own high-frequency ones small. In our experiments, this phenomenon can be widely observed for DNNs of different width (tens to thousands in each layer), depth (one to tens), training algorithms (GD, SGD, Adam), and activation functions (tanh and ReLU). The F-Principle provides insights into the good generalization performance of DNNs often observed in experiments. In Appendix 7, we also discuss how the F-Principle helps understand the training behavior of DNNs in the information plane [18].

Note that initial parameters with large values could complicate the phenomenon of the F-Principle. In previous experiments, the training behavior of DNNs initialized by Gaussian distribution with mean 0 and small standard deviation follows the F-Principle. However, with large initialization, i.e., parameters

initialized by a Gaussian distribution of large standard deviation, it is difficult to observe a clear phenomenon of the F-Principle. More importantly, these two initialization strategies could result in very different generalization performances. When the standard deviation for initialization is large<sup>5</sup>, say, 10 (see Fig.4a), the initial DNN output fluctuates strongly. In contrast, when the parameters of the DNN are initialized with small values, say, Gaussian distribution with standard deviation 0.1, the initial DNN output is flat (see Fig.4d). For both initializations, DNNs can well fit the training data (see Fig.4b and e). However, for test data, the DNN with small initialization generalizes well (Fig.4f) whereas the DNN with large initialization clearly overfits (Fig.4c). Intuitively, the above phenomenon can be understood as follows. Without explicit constraints on the high-frequency components beyond the effective frequency range of the training data, the DNN output after training tends to inherit these high-frequency components from the initial output. Therefore, with large initialization, the DNN output can easily overfit the training data with fluctuating high-frequency components. In practice, the parameters of DNNs are often randomly initialized with standard deviations close to zero. As suggested by our analysis, the small-initialization strategy may implicitly lead to a more efficient and well-generalized optimization process of DNNs as characterized by the F-Principle. Note that a quantitative study of how initialization affects the generalization of DNN can be found in a subsequent work [26].

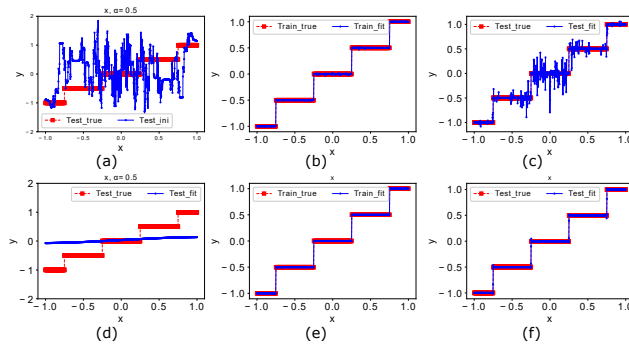


**Fig. 4.** DNN outputs with different initializations for fitting function  $f(x)$  of  $f_0(x) = x$  with  $\alpha = 0.5$  in Eq. (2). The training data and the test data are evenly sampled in  $[-1, 1]$  with sample size 600 and 1200, respectively. The parameters of DNNs are initialized by a Gaussian distribution with mean 0 and standard deviation either 10 (first row) or 0.1 (second row). (a, d):  $f(x)$  (red dashed line) and initial DNN outputs (blue solid line) for the test data. (b, e):  $f(x)$  (red dashed line) and DNN outputs (blue solid line) for the training data at the end of training. (c, f):  $f(x)$  (red dashed line) and DNN outputs (blue solid line) for the test data at the end of training.

<sup>5</sup> The bias terms are always initialized by standard deviation 0.1.



## Acknowledgments

The authors want to thank David W. McLaughlin for helpful discussions and thank Qiu Yang (NYU), Zheng Ma (Purdue University), and Tao Luo (Purdue University), Shixiao Jiang (Penn State), Kai Chen (SJTU) for critically reading the manuscript. Part of this work was done when ZX, YZ, YX are postdocs at New York University Abu Dhabi and visiting members at Courant Institute supported by the NYU Abu Dhabi Institute G1301. The authors declare no conflict of interest.

## References

1. Alain, G., Bengio, Y.: Understanding intermediate layers using linear classifier probes. arXiv preprint arXiv:1610.01644 (2016)
2. Arpit, D., Jastrzebski, S., Ballas, N., Krueger, D., Bengio, E., Kanwal, M.S., Maharaaj, T., Fischer, A., Courville, A., Bengio, Y., et al.: A closer look at memorization in deep networks. arXiv preprint arXiv:1706.05394 (2017)
3. Barnett, A., Greengard, L., Pataki, A., Spivak, M.: Rapid solution of the cryo-em reconstruction problem by frequency marching. *SIAM Journal on Imaging Sciences* **10**(3), 1170–1195 (2017)
4. Cai, W., Li, X., Liu, L.: Phasednn—a parallel phase shift deep neural network for adaptive wideband learning. arXiv preprint arXiv:1905.01389 (2019)
5. Hackbusch, W.: Multi-grid methods and applications, vol. 4. Springer Science and Business Media (2013)
6. Hardt, M., Recht, B., Singer, Y.: Train faster, generalize better: Stability of stochastic gradient descent. arXiv preprint arXiv:1509.01240 (2015)
7. Kawaguchi, K., Kaelbling, L.P., Bengio, Y.: Generalization in deep learning. arXiv preprint arXiv:1710.05468 (2017)
8. Kingma, D.P., Ba, J.: Adam: A method for stochastic optimization. arXiv preprint arXiv:1412.6980 (2014)
9. LeCun, Y., Bengio, Y., Hinton, G.: Deep learning. *nature* **521**(7553), 436 (2015)
10. Lin, J., Camoriano, R., Rosasco, L.: Generalization properties and implicit regularization for multiple passes sgm. In: International Conference on Machine Learning, pp. 2340–2348 (2016)
11. Martin, C.H., Mahoney, M.W.: Rethinking generalization requires revisiting old ideas: statistical mechanics approaches and complex learning behavior. arXiv preprint arXiv:1710.09553 (2017)
12. Mishali, M., Eldar, Y.C.: Blind multiband signal reconstruction: Compressed sensing for analog signals. *IEEE Transactions on Signal Processing* **57**(3), 993–1009 (2009)
13. Percival, D.B., Walden, A.T.: Spectral analysis for physical applications. cambridge university press (1993)
14. Rabinowitz, N.C.: Meta-learners’ learning dynamics are unlike learners’. arXiv preprint arXiv:1905.01320 (2019)

15. Rahaman, N., Arpit, D., Baratin, A., Draxler, F., Lin, M., Hamprecht, F.A., Bengio, Y., Courville, A.: On the spectral bias of deep neural networks. arXiv preprint arXiv:1806.08734 (2018)
16. Saxe, A.M., Bansal, Y., Dapello, J., Advani, M.: On the information bottleneck theory of deep learning. International Conference on Learning Representations (2018)
17. Shannon, C.E.: Communication in the presence of noise. Proceedings of the IRE **37**(1), 10–21 (1949)
18. Shwartz-Ziv, R., Tishby, N.: Opening the black box of deep neural networks via information. arXiv preprint arXiv:1703.00810 (2017)
19. Wu, L., Zhu, Z., E, W.: Towards understanding generalization of deep learning: Perspective of loss landscapes. arXiv preprint arXiv:1706.10239 (2017)
20. Xu, Z.Q.J.: Frequency principle in deep learning with general loss functions and its potential application. arXiv preprint arXiv:1811.10146 (2018)
21. Xu, Z.Q.J., Zhang, Y., Luo, T., Xiao, Y., Ma, Z.: Frequency principle: Fourier analysis sheds light on deep neural networks. arXiv preprint arXiv:1901.06523 (2019)
22. Xu, Z.J.: Understanding training and generalization in deep learning by fourier analysis. arXiv preprint arXiv:1808.04295 (2018)
23. Yen, J.: On nonuniform sampling of bandwidth-limited signals. IRE Transactions on circuit theory **3**(4), 251–257 (1956)
24. Zhang, C., Bengio, S., Hardt, M., Recht, B., Vinyals, O.: Understanding deep learning requires rethinking generalization. arXiv preprint arXiv:1611.03530 (2016)
25. Zhang, Y., Xu, Z.Q.J., Luo, T., Ma, Z.: Explicitizing an implicit bias of the frequency principle in two-layer neural networks. arXiv:1905.10264 [cs, stat] (May 2019), <http://arxiv.org/abs/1905.10264>, arXiv: 1905.10264
26. Zhang, Y., Xu, Z.Q.J., Luo, T., Ma, Z.: A type of generalization error induced by initialization in deep neural networks. arXiv:1905.07777 [cs, stat] (May 2019), <http://arxiv.org/abs/1905.07777>, arXiv: 1905.07777
27. Zhen, H.L., Lin, X., Tang, A.Z., Li, Z., Zhang, Q., Kwong, S.: Nonlinear collaborative scheme for deep neural networks. arXiv preprint arXiv:1811.01316 (2018)
28. Zheng, G., Sang, J., Xu, C.: Understanding deep learning generalization by maximum entropy. arXiv preprint arXiv:1711.07758 (2017)

## 7 Appendix

Through the empirical exploration of the training behavior of DNNs in the information plane, regarding information compression phase, Schwartz-Ziv and Tishby (2017) [18] claimed that (i) information compression is a general process; (ii) information compression is induced by SGD. In this section, we demonstrate how the F-Principle can be used to understand the compression phase.

### 7.1 Computation of information

For any random variables  $U$  and  $V$  with a joint distribution  $P(u, v)$ : the entropy of  $U$  is defined as  $I(U) = -\sum_u P(u) \log P(u)$ ; their mutual information is defined as  $I(U, V) = \sum_{u,v} P(u, v) \log \frac{P(u,v)}{P(u)P(v)}$ ; the conditional entropy of  $U$  on  $V$  is defined as

$$I(U|V) = \sum_{u,v} P(u, v) \log \frac{P(v)}{P(u, v)} = I(U) - I(U, V).$$

By the construction of the DNN, its output  $T$  is a deterministic function of its input  $X$ , thus,  $I(T|X) = 0$  and  $I(X, T) = I(T)$ . To compute entropy numerically, we evenly bin  $X, Y, T$  to  $X_b, Y_b, T_b$  with bin size  $b$  as follows. For any value  $v$ , its binned value is define as  $v_b = \text{Round}(v/b) \times b$ . In our work,  $I(T)$  and  $I(Y, T)$  are approximated by  $I(T_b)$  and  $I(Y_b, T_b)$ , respectively, with  $b = 0.05$ . Note that, after binning, one value of  $X_b$  may map to multiple values of  $T_b$ . Thus,  $I(T_b|X_b) \neq 0$  and  $I(X_b, T_b) \neq I(T_b)$ . The difference vanishes as bin size shrinks. Therefore, with a small bin size,  $I(T_b)$  is a good approximation of  $I(X, T)$ . In experiments, we also find that  $I(X_b, T_b)$  and  $I(T_b)$  behave almost the same in the information plane for the default value  $b = 0.05$ .

## 7.2 Compression vs. no compression in the information plane

We demonstrate how compression can appear or disappear by tuning the parameter  $\alpha$  in Eq. (2) with  $f_0(x) = x$  for  $x \in [-1, 1]$  using full batch gradient descent (GD) without stochasticity. In our simulations, the DNN well fits  $f(x)$  for both  $\alpha$  equal to 0 and 0.5 after training (see Fig.5a and c). In the information plane, there is no compression phase for  $I(T)$  for  $\alpha = 0$  (see Fig.5b). By increasing  $\alpha$  in Eq. (2) we can observe that: i) the fitted function is discretized with only few possible outputs (see Fig.5c); ii) the compression of  $I(T)$  appears (see Fig.5d). For  $\alpha > 0$ , behaviors of information plane are similar to previous results [18]. To understand why compression happens for  $\alpha > 0$ , we next focus on the training courses for different  $\alpha$  in the frequency domain.

A key feature of the class of functions described by Eq. (2) is that the dominant low-frequency components for  $f(x)$  with different  $\alpha$  are the same. By the F-Principle, the DNN first captures those dominant low-frequency components, thus, the training courses for different  $\alpha$  at the beginning are similar, i.e., i) the DNN output is close to  $f_0(x)$  at certain training epochs (blue lines in Fig.5a and c); ii)  $I(T)$  in the information plane increases rapidly until it reaches a value close to the entropy of  $f_0(x)$ , i.e.,  $I(f_0(x))$  (see Fig.5b and d). For  $\alpha = 0$ , the target function is  $f_0(x)$ , therefore,  $I(T)$  will be closer and closer to  $I(f_0(x))$  during the training. For  $\alpha > 0$ , the entropy of the target function,  $I(f(x))$ , is much less than  $I(f_0(x))$ . In the latter stage of capturing high-frequency components, the DNN output  $T$  would converge to the discretized function  $f(x)$ . Therefore,  $I(T)$  would decrease from  $I(f_0(x))$  to  $I(f(x))$ .

This analysis is also applicable to other functions. As the discretization is in general inevitable for classification problems with discrete labels, we can often observe information compression in practice as described in the previous study [18].

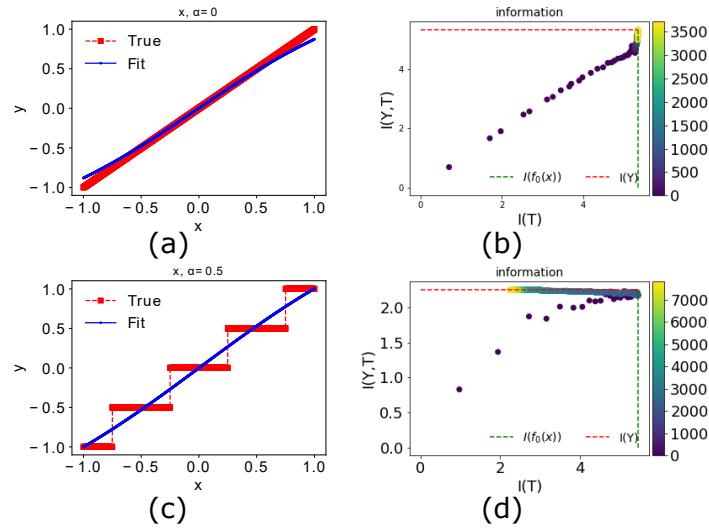


**Fig. 5.** Analysis of compression phase in the information plane.  $\alpha$  is 0 for (a, b) and 0.5 for (c, d). (a, c)  $f(x)$  (red square) with  $f_0(x) = x$  in Eq. (2) and the DNN output (blue solid line) at a certain training step. (b, d) Trajectories of the training process of the DNN in the information plane. Color of each dot indicates its recording step. The green dashed vertical line and the red dashed horizontal line indicate constant values of  $I(f_0(x))$  and  $I(Y)$ , respectively.